

# Accelerating Cross-Validation in Multinomial Logistic Regression with $\ell_1$ -Regularization

Tomoyuki Obuchi

OBUCHI@C.TITECH.AC.JP

Yoshiyuki Kabashima

KABA@C.TITECH.AC.JP

*Department of Mathematical and Computing Science*

*Tokyo Institute of Technology*

*2-12-1, Ookayama, Meguro-ku, Tokyo, Japan*

**Editor:** \*\*\*

## Abstract

We develop an approximate formula for evaluating a cross-validation estimator of predictive likelihood for multinomial logistic regression regularized by an  $\ell_1$ -norm. This allows us to avoid repeated optimizations required for literally conducting cross-validation; hence, the computational time can be significantly reduced. The formula is derived through a perturbative approach employing the largeness of the data size and the model dimensionality. Its usefulness is demonstrated on simulated data and the ISOLET dataset from the UCI machine learning repository.

## 1. Introduction

Multinomial classification is a ubiquitous task. There are several ways to treat this task, such as the naive Bayesian methods, neural networks, decision trees, and hierarchical classification schemes (Trevor et al., 2009). Among them, in this paper, we focus on multinomial logistic regression (MLR), which is simple but powerful enough to be used in many present day applications.

Let us denote each feature vector by  $\mathbf{x}_\mu \in \mathbb{R}^N$  and its class by  $y_\mu \in \{1, \dots, L\}$ . The MLR uses a linear structural model with parameters  $\{\mathbf{w}_a \in \mathbb{R}^N\}_{a=1}^L$  and computes a class- $a$  bias as an overlap:

$$u_{\mu a} = \mathbf{x}_\mu^\top \mathbf{w}_a. \quad (1)$$

A probability such that the feature vector  $\mathbf{x}_\mu$  belongs to the class  $a$  is computed through a softmax function  $\phi$  as:

$$\phi\left(a \mid \{u_{\mu b}\}_{b=1}^L\right) = \frac{e^{u_{\mu a}}}{\sum_{b=1}^L e^{u_{\mu b}}}. \quad (2)$$

These define the MLR.

The maximum likelihood estimation is usually employed to train the MLR in supervised settings, though the learning result tends to be inefficient when the data size is not sufficiently larger than the model dimensionality or noises in relevant levels are present. A common technique to overcome this difficulty is to introduce a penalty or regularization.

In this paper, we use an  $\ell_1$ -regularization, which induces a sparse classifier as a learning result and is accepted to be effective. Given  $M$  data points  $D^M \equiv \{(\mathbf{x}_\mu, y_\mu)\}_{\mu=1}^M$ , the  $\ell_1$ -regularized estimator is defined by the following optimization problem:

$$\begin{aligned} \{\hat{\mathbf{w}}_a(\lambda)\}_a &= \arg \min_{\{\mathbf{w}_a\}_a} \left\{ \sum_{\mu=1}^M q_\mu \left( \{\mathbf{w}_a\}_{a=1}^L \right) + \lambda \sum_{a=1}^L \|\mathbf{w}_a\|_1 \right\} \\ &\equiv \arg \min_{\{\mathbf{w}_a\}_a} \mathcal{H} \left( \{\mathbf{w}_a\}_{a=1}^L \mid D^M, \lambda \right). \end{aligned} \quad (3)$$

where we denote the negative log-likelihood as

$$q_\mu \left( \{\mathbf{w}_a\}_{a=1}^L \right) = -\ln \phi \left( y_\mu \mid \left\{ u_{\mu a} = \mathbf{x}_\mu^\top \mathbf{w}_a \right\}_{a=1}^L \right), \quad (4)$$

and define a regularized cost function or Hamiltonian  $\mathcal{H}$ .

The introduction of regularization causes another problem of model selection or hyperparameter estimation with respect to  $\lambda$ . A versatile framework providing a reasonable estimate is cross-validation (CV), but it has a disadvantage in terms of the computational cost. The literal CV requires repeated optimizations which can be a serious computational burden when the data size and the model dimensionality are large. The purpose of this paper is to resolve this problem by inventing an efficient approximation of CV.

Our technique is based on a perturbative expansion employing the largeness of the data size and the model dimensionality. Similar techniques were also developed for the Bayesian learning of simple perceptrons (Oppen and Winther, 1997), for linear regression with the  $\ell_1$ -regularization (Obuchi and Kabashima, 2016) and with the two-dimensional total variation (Obuchi et al., 2016). Actually, this perturbative approach is fairly general and can be applied to a wide class of generalized linear models with simple convex regularizations. For example in the present MLR case, it is easy to extend our result to the case where both the  $\ell_1$ - and  $\ell_2$ -regularizations exist, which is used in a common implementation (Friedman et al., 2010). The derivation of our approximate formula below is, however, conducted on the case of the  $\ell_1$ -regularization only, for simplicity. The extension to the mixed regularization case is briefly stated after the derivation.

The rest of the paper is organized as follows. In sec. 2, we state our formulation and how to derive the approximate formula. In sec. 3, we compare our approximation result with that of the literally conducted CV on simulated data and on the ISOLET dataset from UCI machine learning repository (Lichman, 2013). The accuracy and the computational time of our approximate formula are reported in comparison with the literal CV. The last section is devoted to the conclusion.

## 2. Formulation

In the maximum likelihood estimation framework, it is natural to employ a predictive likelihood as a criterion for model selection (Bjornstad, 1990; Ando and Tsay, 2010). We require a good estimator of the predictive likelihood, and the CV provides a simple realization of it. Particularly in this paper, we consider an estimator based on the leave-one-out (LOO)

CV. The LOO solution is described by

$$\{\hat{\mathbf{w}}_a^{\setminus\mu}(\lambda)\}_a = \arg \min_{\{\mathbf{w}_a\}_a} \left\{ \mathcal{H} \left( \{\mathbf{w}_a\}_{a=1}^L \middle| D^M, \lambda \right) - q_\mu \left( \{\mathbf{w}_a\}_{a=1}^L \right) \right\} \equiv \arg \min_{\{\mathbf{w}_a\}_a} \left\{ \mathcal{H}^{\setminus\mu} \right\}. \quad (5)$$

Denoting the overlap of  $\mathbf{x}_\mu$  with the LOO solution as  $\hat{u}_{\mu a}^{\setminus\mu} = \mathbf{x}_\mu^\top \hat{\mathbf{w}}_a^{\setminus\mu}$ , as well as that with the full solution  $\hat{u}_{\mu a} = \mathbf{x}_\mu^\top \hat{\mathbf{w}}_a$ , we can define the LOO estimator (LOOE) of the predictive likelihood as:

$$\epsilon_{\text{LOO}}(\lambda) = \frac{1}{M} \sum_{\mu=1}^M q_\mu \left( \left\{ \hat{\mathbf{w}}_a^{\setminus\mu} \right\}_{a=1}^L \right) = -\frac{1}{M} \sum_{\mu=1}^M \ln \phi \left( y_\mu \middle| \{\hat{u}_{\mu a}^{\setminus\mu}\}_{a=1}^L \right). \quad (6)$$

The minimum of the LOOE determines the optimal value of  $\lambda$  though its evaluation requires us to solve eq. (5)  $M$  times, which is computationally demanding.

### 2.0.1 NOTATIONS

Here, we fix the notations for a better flow of the derivation shown below. By summarizing the class index, we introduce a vector notation of the overlap as  $\mathbf{u}_\mu = (u_{\mu a})_a \in \mathbb{R}^L$  and an extended vector representation of the weight vectors  $\{\mathbf{w}_a\}_a$  as  $\mathbf{W} = (\mathbf{w}_a)_a \in \mathbb{R}^{LN}$ . The  $m$ th component of  $\mathbf{W}$  can thus be decomposed into two parts as  $m = (m_c, m_f)$  where  $m_c \in \{1, \dots, L\}$  denotes the class index and  $m_f \in \{1, \dots, N\}$  represents the component index of the feature vector. Namely we write  $W_m = w_{m_c m_f}$ . Correspondingly, we leverage a matrix  $X^\mu \in \mathbb{R}^{L \times LN}$  to define a repetition representation of the feature vector  $\mathbf{x}_\mu$ : Each component is defined as:

$$X_{am}^\mu \equiv \delta_{am_c} x_{\mu m_f}. \quad (7)$$

This yields simple and convenient relations:

$$\mathbf{u}_\mu = X^\mu \mathbf{W}, \quad X^\mu = \left( \frac{\partial \mathbf{u}_\mu}{\partial \mathbf{W}} \right)^\top. \quad (8)$$

Further, the class- $a$  probability of  $\mu$ th data at the full solution  $\hat{\mathbf{W}} = (\hat{\mathbf{w}}_a)_a$  is denoted by:

$$p_{a|\mu} = \phi(a | \{\hat{u}_{\mu b}\}_b) = \frac{e^{\hat{u}_{\mu a}}}{\sum_{b=1}^L e^{\hat{u}_{\mu b}}} \quad (9)$$

These notations express the gradient and the Hessian of  $q_\mu$  at the full solution as:

$$\nabla q_\mu(\hat{\mathbf{W}}) \equiv \frac{\partial q_\mu}{\partial \mathbf{W}} \Big|_{\mathbf{W}=\hat{\mathbf{W}}} = \frac{\partial \mathbf{u}_\mu}{\partial \mathbf{W}} \frac{\partial}{\partial \mathbf{u}_\mu} q_\mu \Big|_{\mathbf{u}_\mu=\hat{\mathbf{u}}_\mu} = (X^\mu)^\top \mathbf{b}^\mu, \quad (10)$$

$$\begin{aligned} \partial^2 q_\mu(\hat{\mathbf{W}}) &\equiv \frac{\partial^2 q_\mu}{\partial \mathbf{W} \partial \mathbf{W}'} \Big|_{\mathbf{W}=\mathbf{W}'=\hat{\mathbf{W}}} \\ &= \frac{\partial \mathbf{u}_\mu}{\partial \mathbf{W}} \left( \frac{\partial^2 q_\mu}{\partial \mathbf{u}_\mu \partial \mathbf{u}'_\mu} \Big|_{\mathbf{u}_\mu=\mathbf{u}'_\mu=\hat{\mathbf{u}}_\mu} \right) \left( \frac{\partial \mathbf{u}'_\mu}{\partial \mathbf{W}'} \right)^\top = (X^\mu)^\top F^\mu X^\mu, \end{aligned} \quad (11)$$

where

$$\mathbf{b}^\mu \equiv (p_{1|\mu} - \delta_{1y_\mu}, p_{2|\mu} - \delta_{2y_\mu}, \dots, p_{L|\mu} - \delta_{Ly_\mu})^\top, \quad (12)$$

$$F_{ab}^\mu \equiv \delta_{ab} p_{a|\mu} - p_{a|\mu} p_{b|\mu}. \quad (13)$$

In addition, we denote the cost function Hessians at the respective solutions as:

$$G \equiv \partial^2 \mathcal{H}(\hat{\mathbf{W}}) = \sum_{\mu} \left( \partial^2 q_{\mu}(\hat{\mathbf{W}}) \right), \quad (14)$$

$$G^{\setminus\mu} \equiv \partial^2 \mathcal{H}^{\setminus\mu}(\hat{\mathbf{W}}^{\setminus\mu}) = G - \partial^2 q_{\mu}(\hat{\mathbf{W}}^{\setminus\mu}). \quad (15)$$

Finally, we introduce the symbol  $A(\mathbf{W}) = \{m | W_m \neq 0\}$  representing the index set of the active components of  $\mathbf{W}$  and  $\hat{A} = A(\hat{\mathbf{W}})$ . Given  $\hat{\mathbf{W}}$ , we denote the active components of a vector  $\mathbf{Y} \in \mathbb{R}^{LN}$  by the subscript as  $\mathbf{Y}_{\hat{A}}$ . A similar notation is used for any matrix and the symbol  $*$  is assumed to represent all of the components in the corresponding dimension.

## 2.1 Approximate formula

For a simple derivation, it is important to consider that the  $\mathbf{w}$  dependence of  $\phi$  appears only in the overlap  $u = \mathbf{x}^\top \mathbf{w}$ . Hence, it is sufficient to provide the relation between  $\hat{u}_{\mu a}$  and  $\hat{u}_{\mu a}^{\setminus\mu}$  in order to derive the approximate formula.

A crucial assumption to derive the formula is that the active set is ‘‘common’’ between the full and LOO solutions,  $\hat{\mathbf{W}} = (\hat{w}_a)_a$  and  $\hat{\mathbf{W}}^{\setminus\mu} = (\hat{w}_a^{\setminus\mu})_a$ ; namely  $\hat{A} = \hat{A}^{\setminus\mu} \equiv A(\hat{\mathbf{W}}^{\setminus\mu})$ . Although this assumption is literally not true, we numerically confirmed that this approximately holds. In other words, the change of the active set is small enough compared to the size of the active set itself when considering the LOO operation when  $N$  and  $M$  are large. Moreover, in a related problem of an  $\ell_1$ -regularized linear regression, the so-called LASSO, it has been shown that the contribution of the active set change vanishes in a limit  $N, M \rightarrow \infty$  keeping  $\alpha = M/N = O(1)$  (Obuchi and Kabashima, 2016). It is expected that the same holds in the present problem. Hence, we adopt this assumption in the following definition.

Once the active set  $\hat{A}$  is assumed to be known and unchanged by the LOO operation, it is easy to determine the active components of the full and LOO solutions  $\hat{\mathbf{W}}$  and  $\hat{\mathbf{W}}^{\setminus\mu}$ . The vanishing condition of the gradient of the cost function is the determining equation:

$$(\nabla \mathcal{H})_{\hat{A}} = 0 \Rightarrow \hat{\mathbf{W}}_{\hat{A}}, \quad (16)$$

$$\left( \nabla \mathcal{H}^{\setminus\mu} \right)_{\hat{A}} = (\nabla \mathcal{H})_{\hat{A}} - (\nabla q_{\mu})_{\hat{A}} = 0 \Rightarrow \hat{\mathbf{W}}_{\hat{A}}^{\setminus\mu}. \quad (17)$$

The difference between the gradients is only  $\nabla q_{\mu}$ , and hence the difference between  $\hat{\mathbf{W}}$  and  $\hat{\mathbf{W}}^{\setminus\mu}$  is expected to be small. Denoting the difference as  $\mathbf{d}^\mu = \hat{\mathbf{W}} - \hat{\mathbf{W}}^{\setminus\mu}$  and expanding eq. (17) with respect to  $\mathbf{d}^\mu$  up to the first order, we obtain an equation determining  $\mathbf{d}^\mu$ :

$$\mathbf{d}_{\hat{A}}^\mu = - \left( G_{\hat{A}\hat{A}}^{\setminus\mu} \right)^{-1} \left( \nabla q_{\mu}(\hat{\mathbf{W}}) \right)_{\hat{A}}. \quad (18)$$

Inserting this and eq. (10) into the definition  $\mathbf{d}^\mu = \hat{\mathbf{W}} - \hat{\mathbf{W}}^{\setminus\mu}$  and multiplying  $X^\mu$  from left, we obtain:

$$\hat{\mathbf{u}}_{\mu}^{\setminus\mu} \approx \hat{\mathbf{u}}_{\mu} + X_{*\hat{A}}^\mu \left( G_{\hat{A}\hat{A}}^{\setminus\mu} \right)^{-1} \left( X_{*\hat{A}}^\mu \right)^\top \mathbf{b}^\mu \equiv \hat{\mathbf{u}}_{\mu} + C_{\mu}^{\setminus\mu} \mathbf{b}^\mu. \quad (19)$$

This equation implies that the matrix inversion operation is necessary for each  $\mu$ , which still requires a significant computational cost. To avoid this, we employ an approximation and the Woodbury matrix inversion formula in conjunction with eqs. (11,14) and (15). The result is:

$$\begin{aligned} (G^{\setminus\mu})^{-1} &\equiv (\partial^2 \mathcal{H}^{\setminus\mu}(\hat{\mathbf{W}}^{\setminus\mu}))^{-1} \approx (\partial^2 \mathcal{H}^{\setminus\mu}(\hat{\mathbf{W}}))^{-1} = (G - (X^\mu)^\top F^\mu X^\mu)^{-1} \\ &= G^{-1} - G^{-1} (X^\mu)^\top \left( -F^\mu + X^\mu G^{-1} (X^\mu)^\top \right)^{-1} X^\mu G^{-1}. \end{aligned} \quad (20)$$

Inserting this into eq. (19) and simplifying several factors, we obtain:

$$\hat{\mathbf{u}}_\mu^{\setminus\mu} \approx \hat{\mathbf{u}}_\mu + C_\mu (I_L - F^\mu C_\mu)^{-1} \mathbf{b}^\mu, \quad (21)$$

where

$$C_\mu = X_{*\hat{A}}^\mu (G_{\hat{A}\hat{A}})^{-1} (X_{*\hat{A}}^\mu)^\top. \quad (22)$$

Now, all of the variables on the righthand side of eq. (21) can be computed from the full solution  $\hat{\mathbf{W}}$  only, which enables us to estimate the LOOE by leveraging a one-time optimization using all of the data  $D^M$ , while avoiding repeated optimizations.

We should mention the computational cost of this approximation: it is mainly scaled as  $O(ML^2|\hat{A}| + ML|\hat{A}|^2 + |\hat{A}|^3)$ . The first two terms come from the construction of  $G_{\hat{A}\hat{A}}$  and  $C_\mu$ , and the last one is derived from the inverse of  $G$ . If  $|\hat{A}|$  is proportional to the feature dimensionality  $N$ , this computational cost is of the third order with respect to the system dimensionality  $N$  and  $M$ . This is admittedly not cheap and the computational cost for the  $k$ -fold literal CV with a moderate value of  $k$  becomes smaller than that for our approximation in a large dimensionality limit. We, however, stress that there actually exists a wide range of  $N$  and  $M$  values in which our approximation outperforms the literal CV in terms of the computational time, as later demonstrated in sec. 3. Moreover, when treating much larger systems, we invent a further simplified approximation based on the above approximate formula. The computational cost of this simplified version is scaled only linearly with respect to the system dimensionality. Its derivation is in sec. 2.2 and the precision comparison to the original approximation is in sec. 3.

Another sensitive issue is present in computing  $(G_{\hat{A}\hat{A}})^{-1}$ . Occasionally the cost function Hessian  $G$  has zero eigenvalues and is not invertible. We handle this problem in the next subsection.

### 2.1.1 HANDLING ZERO MODES

In the MLR, there is an intrinsic symmetry such that the model is invariant under the addition of any constant vector to the weight vectors of all classes:

$$\mathbf{w}_a \rightarrow \mathbf{w}_a + \mathbf{v} \quad (\forall a). \quad (23)$$

In this sense, the weight vectors defining the same model are ‘‘degenerated’’ and our MLR is singular. For finite  $\lambda$ , this is not harmful because the regularization term resolves this singularity and selects an optimal one  $\{\hat{\mathbf{w}}_a\}_a$  with the smallest value of  $\|\mathbf{w}_a\|_1$  among the

degenerated vectors. However, this does not mean that the associated Hessian is non-singular. The regularization term does not provide any direct contribution to the Hessian and as a result, the Hessian tends to have some zero modes. This prevents taking the inverse Hessian  $G^{-1}$  in eq. (22). How can we overcome this?

One possibility is to fix the weights of one certain class at constant values when solving the optimization problem (3). This is termed ‘‘gauge fixing’’ in physics, and one convenient gauge in the present problem will be the zero gauge in which the weights in a chosen class are fixed at zeros. This is actually found in some earlier implementations (Krishnapuram et al., 2005; Schmidt, 2010) and is preferable for our approximate formula because it removes the harmful zero modes of the Hessian from the beginning. However, some other implementations which are currently well accepted do not employ such gauge fixing (Friedman et al., 2010), and moreover even with gauge fixing very small eigenvalues sometimes accidentally emerge in the Hessian. Hence, for user convenience, we require another way of avoiding this problem.

Another possibility is to remove the zero modes by hand. By construction, the zero modes are associated to the model invariance. This implies that those zero modes are irrelevant and may be removed. In fact, we are only interested in the perturbations which truly change the model, and the modes which maintain the model unchanged are unnecessary. According to this consideration, we replace  $G^{-1}$  in eq. (22) with the zero-mode-removed inverse Hessian  $\overline{G}^{-1}$ . The computation of  $\overline{G}^{-1}$  is straightforward: we perform the eigenvalue decomposition of  $G_{\hat{A}\hat{A}}$  and obtain the eigenvalues:  $\{d_i\}_{i=1}^{|\hat{A}|}$  and eigenvectors:  $\{\mathbf{v}_i\}_{i=1}^{|\hat{A}|}$ , which allows us to represent

$$G_{\hat{A}\hat{A}} = \sum_i d_i \mathbf{v}_i \mathbf{v}_i^\top = \sum_{i \in S^+} d_i \mathbf{v}_i \mathbf{v}_i^\top, \quad (24)$$

where  $S^+$  denotes the index set of the modes with finite eigenvalues. Then,  $\overline{G}^{-1}$  is defined as:

$$\overline{G}_{\hat{A}\hat{A}}^{-1} \equiv \sum_{i \in S^+} d_i^{-1} \mathbf{v}_i \mathbf{v}_i^\top. \quad (25)$$

Finally, we replace  $G^{-1}$  by  $\overline{G}^{-1}$  in eq. (22), and obtain:

$$C_\mu = X_{*\hat{A}}^\mu \overline{G}_{\hat{A}\hat{A}}^{-1} \left( X_{*\hat{A}}^\mu \right)^\top. \quad (26)$$

By using this instead of eq. (22), the problem caused by the zero modes can be avoided.

### 2.1.2 EXTENSION TO THE MIXED REGULARIZATION CASE

Let us briefly state how we can generalize the present result to the case of the mixed regularizations of the  $\ell_1$ - and  $\ell_2$ -terms. The problem to be solved can be defined as follows:

$$\{\hat{\mathbf{w}}_a(\lambda_1, \lambda_2)\}_a = \arg \min_{\{\mathbf{w}_a\}_a} \left\{ \sum_{\mu=1}^M q_\mu \left( \{\mathbf{w}_a\}_{a=1}^L \right) + \lambda_1 \sum_{a=1}^L \|\mathbf{w}_a\|_1 + \frac{\lambda_2}{2} \sum_{a=1}^L \|\mathbf{w}_a\|_2^2 \right\}. \quad (27)$$

where  $\|\cdot\|_2$  denotes the  $\ell_2$  norm. Following the derivation in sec. 2.1, we realize that the derivation is essentially the same, and the difference only appears in the cost function Hessian:

$$G_{\text{mxd}} = \sum_{\mu} \left( \partial^2 q_{\mu}(\hat{\mathbf{W}}) \right) + \lambda_2 I_{NL}, \quad (28)$$

where  $I_{NL}$  is the identity matrix of size  $NL$ . As a result, we can compute the LOO solution by leveraging the same equation as eq. (21) by replacing the definition of  $C_{\mu}$ , eq. (22), with:

$$C_{\mu} = X_{*\hat{A}}^{\mu} \left( (G_{\text{mxd}})_{\hat{A}\hat{A}} \right)^{-1} \left( X_{*\hat{A}}^{\mu} \right)^{\top}. \quad (29)$$

Thanks to the  $\ell_2$  term, the zero mode removal is not needed since the eigenvalues are lifted up by  $\lambda_2$ .

### 2.1.3 BINOMIAL CASE

The binomial case  $L = 2$  is particularly interesting in several applications and thus we write down the specific formula for this case.

In the binomial case, it is fairly common to express the class  $y$  as a binary  $y = 0, 1$  and to use the following logit function:

$$\phi_{\text{logit}}(y_{\mu}|u_{\mu}) = \frac{\delta_{y_{\mu}1} + \delta_{y_{\mu}0}e^{-u_{\mu}}}{1 + e^{-u_{\mu}}}, \quad (30)$$

where

$$u_{\mu} = \mathbf{x}_{\mu}^{\top} \mathbf{w}. \quad (31)$$

If we identify  $y = 0$  in this case as  $y = 1$  in the two-class MLR case, this is nothing but the two-class MLR with a zero gauge  $\mathbf{w}_1 = \mathbf{0}$ . Hence, there is no harmful zero mode in the Hessian and we can naively apply our approximate formula. The explicit form in this case is:

$$\hat{u}_{\mu}^{\setminus\mu} \approx \hat{u}_{\mu} + \frac{c^{\mu}}{1 - \frac{\partial^2 q_{\mu}}{\partial u_{\mu}^2} c^{\mu}} \frac{\partial q_{\mu}}{\partial u_{\mu}}, \quad (32)$$

where  $q_{\mu} = -\ln \phi_{\text{logit}}(y_{\mu}|u_{\mu})$  and

$$\frac{\partial q_{\mu}}{\partial u_{\mu}} = \delta_{y_{\mu}0} - \frac{e^{-u_{\mu}}}{1 + e^{-u_{\mu}}}, \quad (33)$$

$$\frac{\partial^2 q_{\mu}}{\partial u_{\mu}^2} = \frac{e^{-u_{\mu}}}{(1 + e^{-u_{\mu}})^2}, \quad (34)$$

$$G_{\hat{A}\hat{A}} = \sum_{\mu=1}^M \frac{\partial^2 q_{\mu}}{\partial u_{\mu}^2} \left( \mathbf{x}_{\mu} \mathbf{x}_{\mu}^{\top} \right)_{\hat{A}\hat{A}}, \quad (35)$$

$$c^{\mu} = \left( \mathbf{x}_{\mu}^{\top} \right)_{\hat{A}} \left( G_{\hat{A}\hat{A}} \right)^{-1} \left( \mathbf{x}_{\mu} \right)_{\hat{A}}, \quad (36)$$

and  $\hat{A} = \{i | \hat{w}_i \neq 0\}$  is the active set of the full solution, as before.

Note that this approximation can be easily generalized to arbitrary differentiable output functions by replacing the logit function  $\phi_{\text{logit}}$ . Readers are thus encouraged to implement approximate CVs in a variety of different problems.

## 2.2 Further simplified approximation

As mentioned above, the computational cost of our approximation is  $O(ML^2|\hat{A}| + ML|\hat{A}|^2 + |\hat{A}|^3)$  and should be reduced for treating larger systems. For this, we derive a further simplified approximation based on the invented approximate formula above. We call this a self-averaging (SA) approximation according to physics terminology.

The basic idea for simplifying our approximate formula is to assume a weak ‘‘correlation’’ between  $W_m$  and  $W_n$ . The meaning of ‘‘correlation’’ is not evident here, but as seen in sec. A the Hessian  $G$  can be connected to a (rescaled) covariance  $\chi$  between  $W_m$  and  $W_n$  in a statistical mechanical formulation introducing a probability distribution of  $\mathbf{W}$ . In this way, the Hessian is assumed to be expressed in a rather restricted form:

$$(G^{\setminus\mu})_{mn}^{-1} \approx \begin{cases} (\chi_{m_f})_{m_c n_c} \delta_{m_f n_f}, & (m, n \in \hat{A}) \\ 0, & (\text{otherwise}) \end{cases}, \quad (37)$$

where  $m_c (= 1, \dots, L)$  is the class index and  $m_f (= 1, \dots, N)$  is the feature component index defined thus far. Namely, the SA Hessian is allowed to take finite values if and only if the two indices share the same feature vector component and its  $\mu$ -dependence is negligible.

To proceed with the computation, we require a closed equation to determine the  $L \times L$  matrix  $\chi_i$  for  $i = 1, \dots, N$ . Its derivation is rather technical and is deferred to sec. A. The result is:

$$(\chi_i)_{\hat{A}_i \hat{A}_i} = \frac{1}{\sigma_x^2} \left( \sum_{\nu=1}^M \left( (I_L + F^\nu C_{\text{SA}})^{-1} F^\nu \right)_{\hat{A}_i \hat{A}_i} \right)^{-1}, \quad (38)$$

where  $\sigma_x^2 = \sum_\mu \sum_i x_{\mu i}^2 / (NM)$  and  $\hat{A}_i = \{a | \hat{w}_{ai} \neq 0\}$  is the set of active class variables at the feature component  $i$ ; the other components of  $\chi_i$  related to inactive components are zeros. The SA approximation of  $C_\mu^{\setminus\mu}$ ,  $C_{\text{SA}} \in \mathbb{R}^{L \times L}$ , is defined by:

$$C_{\text{SA}} = \sigma_x^2 \sum_{i=1}^N \chi_i. \quad (39)$$

Using the solution of eqs. (38,39), the approximate formula is now simply expressed as:

$$\hat{\mathbf{u}}_\mu^{\setminus\mu} \approx \hat{\mathbf{u}}_\mu + C_{\text{SA}} \mathbf{b}^\mu. \quad (40)$$

Note that there is no factor like  $(I_L - F^\mu C_\mu)^{-1}$  in contrast to eq. (21), because we directly approximate  $C_\mu^{\setminus\mu}$  in eq. (19).

When solving eqs. (38,39), the inverse at the right-hand side of eq. (38) becomes occasionally ill-defined again due to the presence of zero modes. In such cases, we should remove the zero modes as eq. (25). Putting  $R = \sum_{\mu=1}^M \left( (I_L + F^\mu C_{\text{SA}})^{-1} F^\mu \right)$  and performing the eigenvalue decomposition, we define its zero-mode-removed inverse  $\bar{R}^{-1}$  as:

$$R_{\hat{A}_i \hat{A}_i} = \sum_j d_j \mathbf{v}_j \mathbf{v}_j^\top = \sum_{j \in S^+} d_j \mathbf{v}_j \mathbf{v}_j^\top \Rightarrow \bar{R}_{\hat{A}_i \hat{A}_i}^{-1} = \sum_{j \in S^+} d_j^{-1} \mathbf{v}_j \mathbf{v}_j^\top, \quad (41)$$



where  $S^+$  is the index set of the modes with finite eigenvalues. This requires a  $O(L^3)$  computational cost at a maximum. Leveraging this approach, a naive way to solve eqs. (38,39) is a recursive substitution. If this converges in a constant time, irrespectively of the system parameters  $N, M$  and  $L$ , then the computational cost of the SA approximation is scaled as  $O(NL^3 + ML^3)$ . This is linear in the feature dimensionality  $N$  and the data size  $M$  and hence, its advantage is significant.

### 2.3 Summary of procedures

Here, we summarize the two versions of the approximation derived thus far as algorithmic procedures. We call the first version, based on eq. (21), the approximate CV or ACV, and call the second one, using eq. (40), the self-averaging approximate CV or SAACV. The procedures of ACV and SAACV are given in Alg. 1 and Alg. 2, respectively. Comments

---

#### Algorithm 1 Approximate CV of the MLR

---

```

1: procedure ACV( $\hat{\mathbf{W}}(\lambda), D^M$ )
2:   Compute the active set  $\hat{A}$  from  $\hat{\mathbf{W}}$ 
3:   Compute  $\{\hat{\mathbf{u}}_\mu, X^\mu, \mathbf{b}^\mu, F^\mu\}_\mu$  by eqs. (1,7), (12) and (13)
4:    $G_{\hat{A}\hat{A}} \leftarrow \sum_{\mu=1}^M (X^\mu)^\top F^\mu X^\mu$   $\triangleright O(ML|\hat{A}|^2 + ML^2|\hat{A}|)$ 
5:   Compute  $\overline{G}_{\hat{A}\hat{A}}^{-1}$  by eq. (25)  $\triangleright O(|\hat{A}|^3)$ 
6:   for  $\mu = 1, \dots, M$  do  $\triangleright O(ML|\hat{A}|^2 + ML^2|\hat{A}| + ML^3)$ 
7:      $C_\mu \leftarrow X_{*\hat{A}}^\mu \overline{G}_{\hat{A}\hat{A}}^{-1} (X_{*\hat{A}}^\mu)^\top$ 
8:      $\hat{\mathbf{u}}_\mu^\mu \leftarrow \hat{\mathbf{u}}_\mu + C_\mu (I_L - F^\mu C_\mu)^{-1} \mathbf{b}^\mu$ 
9:   end for
10:  Compute  $\epsilon_{\text{LOO}}$  from  $\{\mathbf{u}_\mu^\mu\}_\mu$  by eq. (6)
11:  return  $\epsilon_{\text{LOO}}$ 
12: end procedure

```

---

are added for specifying the time consuming parts in the entire procedures. In Alg. 2, we describe an actual implementation for solving  $C_{\text{SA}}$  by recursion, which is not fully specified in sec. 2.2. The symbol  $\|\cdot\|_{\text{F}}$  denotes the Frobenius norm and we set the threshold  $\theta$  judging the convergence as  $\theta = 10^{-8}$  in typical situations.

### 3. Numerical experiments

In this section, we examine the precision and actual computational time of ACV and SAACV in numerical experiments. Both simulated and actual datasets (from UCI machine learning repository, Lichman, 2013) are used.

For examination, we compute another predictive likelihood estimator by literally conducting a 10-fold CV, and compare it to the result of our approximate formula. Moreover, as a reference, we compute the likelihood of the full solution  $\{\hat{\mathbf{w}}_a\}_{a=1}^L$  as:

$$\epsilon = \frac{1}{M} \sum_{\mu=1}^M q_\mu \left( \{\hat{\mathbf{w}}_a\}_{a=1}^L \right), \quad (42)$$

---

**Algorithm 2** Self-averaging approximate CV of the MLR

---

```

1: procedure SAACV( $\hat{\mathbf{W}}(\lambda), D^M$ )
2:   Compute the active sets  $\{\hat{A}_i\}_{i=1}^N$  from  $\hat{\mathbf{W}}$ 
3:   Compute  $\{\mathbf{u}_\mu, X^\mu, \mathbf{b}_\mu, F^\mu\}_\mu$  by eqs. (1,7), (12) and (13)
4:    $t \leftarrow 0$  ▷ Start initialization
5:   for  $i = 1, \dots, N$  do
6:      $(\chi_i^{\setminus \mu})^{(t)} \leftarrow 0$ ,
7:      $(\chi_i^{\setminus \mu})_{\hat{A}_i \hat{A}_i}^{(t)} \leftarrow \sigma_x^{-2}$ ,
8:   end for
9:    $\Delta \leftarrow 100$  ▷ End initialization
10:  while  $\Delta > \theta$  do ▷ Compute  $C_{\text{SA}}$  by recursion
11:     $C_{\text{SA}}^{(t+1)} \leftarrow \sigma_x^2 \sum_{i=1}^N (\chi_i^{\setminus \mu})^{(t)}$ 
12:     $R \leftarrow \sum_{\mu=1}^M (I_L + F^\mu C_{\text{SA}}^{(t+1)})^{-1} F^\mu$  ▷  $O(ML^3)$ 
13:     $\Delta \leftarrow 0$ 
14:    for  $i = 1, \dots, N$  do ▷  $O(NL^3)$ 
15:      Compute  $\bar{R}_{\hat{A}_i \hat{A}_i}^{-1}$  by eq. (41) from  $R$ 
16:       $(\chi_i^{\setminus \mu})_{\hat{A}_i \hat{A}_i}^{(t+1)} \leftarrow \sigma_x^{-2} \bar{R}_{\hat{A}_i \hat{A}_i}^{-1}$ 
17:       $\Delta \leftarrow \Delta + \left\| (\chi_i^{\setminus \mu})_{\hat{A}_i \hat{A}_i}^{(t+1)} - (\chi_i^{\setminus \mu})_{\hat{A}_i \hat{A}_i}^{(t)} \right\|_F$ 
18:    end for
19:     $\Delta \leftarrow \Delta/N$ 
20:     $t \leftarrow t + 1$ 
21:  end while
22:  for  $\mu = 1, \dots, M$  do
23:     $\mathbf{u}_\mu^{\setminus \mu} \leftarrow \mathbf{u}_\mu + C_{\text{SA}}^{(t)} \mathbf{b}^\mu$ 
24:  end for
25:  Compute  $\epsilon_{\text{LOO}}$  from  $\{\mathbf{u}_\mu^{\setminus \mu}\}_\mu$  by eq. (6)
26:  return  $\epsilon_{\text{LOO}}$ 
27: end procedure

```

---

and call it the training likelihood, hereafter. The training likelihood is expected to be a monotonic increasing function with respect to  $\lambda$ , while the predictive one is supposed to be non-monotonic.

In all of the experiments defined below, we used a single CPU of Intel(R) Xeon(R) E5-2630 v3 2.4GHz. To solve the optimization problems in eqs. (3,5), we employed *Glmnet* (Friedman et al., 2010) which is implemented as a *MEX* subroutine in MATLAB<sup>®</sup>. The two approximations were implemented as raw codes in MATLAB. This is not the most optimized approach, because as seen in Algs. 1,2 our approximate formula uses a number of *for* and *while* loops which are slow in MATLAB, and hence the comparison is not necessarily fair. However, even in this comparison there is a significant difference in the computational time between the literal CV and our approximations, as shown below.

A sensitive point which should be noted is the convergence problem of the algorithm for solving the present optimization problem. In *Glmnet*, a specialized version of coordinate descent methods is employed, and it requires a threshold  $\delta$  to judge the algorithm convergence. Unless explicitly mentioned, we set this as  $\delta = 10^{-8}$  being tighter than the default value. This is necessary since we treat problems of rather large sizes. A looser choice for  $\delta$  rather strongly affects the literal CV result, while it does not change the full solution or the training likelihood as much. As a result, our approximations employing only the full solution are rather robust against the choice of  $\delta$  compared to the literal CV. This is also demonstrated below.

### 3.1 On simulated dataset

Let us start by testing with the simulated data. Suppose each “true” feature vector  $\mathbf{w}_{0a}$  is independently identically drawn (i.i.d.) from the following Bernoulli-Gaussian prior:

$$\mathbf{w}_{0a} \sim \prod_{i=1}^N \{(1 - \rho_0)\delta(v_{ai}) + \rho_0\mathcal{N}(0, 1/\rho_0)\}, \quad (43)$$

where  $\mathcal{N}(\mu, \sigma^2)$  denotes a Gaussian distribution whose mean and variance are  $\mu$  and  $\sigma^2$ , respectively. The resultant feature vector  $\mathbf{v}_a$  becomes  $N\rho_0$  ( $\equiv K_0$ )-sparse and its norm becomes  $\sqrt{N}$  on average. Then, we choose a class  $y_\mu$  from  $\{1, \dots, L\}$  uniformly and randomly, and generate an observed feature vector  $\mathbf{x}_\mu$  by leveraging the following linear process:

$$\mathbf{x}_\mu = \frac{\mathbf{w}_{0y_\mu}}{\sqrt{N}} + \boldsymbol{\xi}, \quad (44)$$

where  $\boldsymbol{\xi}$  is an observation noise each component of which is i.i.d. from a Gaussian  $\mathcal{N}(0, \sigma_N^2)$ .

For convenience, we introduce the ratio of the data size to the feature dimensionality,  $\alpha = M/N$ , and now obtain five parameters  $\{N, L, \alpha, \rho_0, \sigma_\xi^2\}$  characterizing the experimental setup. It is rather heavy to obtain the dependence of all parameters and below, we mainly focus on the dependence on  $L$ ,  $\sigma_\xi^2$ , and  $N$ . Other parameters are set to be  $\alpha = 2$  and  $\rho_0 = 0.5$ .

#### 3.1.1 RESULT

Let us summarize the result on simulated data.

Fig. 1 shows the plots of the predictive and training likelihoods against  $\lambda$  for  $L = 4, 8, 16$  at  $N = 200$  and  $\sigma_\xi^2 = 0.01$ . This demonstrates that both approximations provide consistent

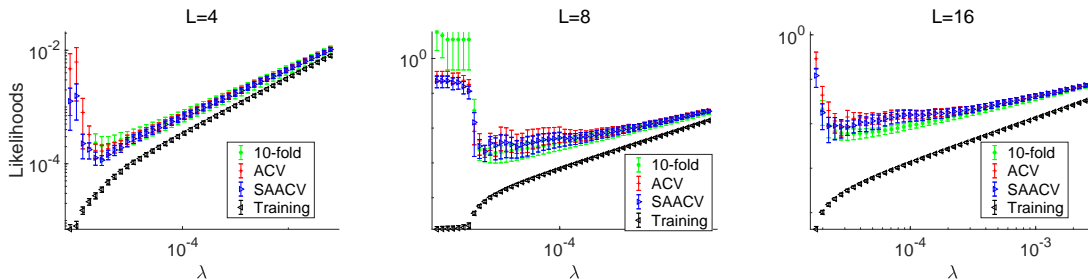


Figure 1: Log-log plots of the likelihoods against  $\lambda$  for several values of the class number  $L$ . Other parameters are fixed at  $N = 200$ ,  $\sigma_\xi^2 = 0.01$ ,  $\alpha = 2$  and  $\rho_0 = 0.5$ . The approximation results are consistent with the literal 10-fold CV results, except at small  $\lambda$ s for small  $L(= 4, 8)$ , which is presumably due to a numerical instability occurring in the literal CV at small  $\lambda$ s.

results with the literal 10-fold CV, except at small  $\lambda$ s for small  $L(= 4, 8)$ . This inconsistency at small  $\lambda$ s is considered to be due to a numerical instability occurring in the literal CV. Actually, for small  $\lambda$ s, we have observed that certain small changes in the data induce large differences in the literal CV result. This example demonstrates that our approximations provide robust curves even in such situations. Note that as  $L$  grows the number of estimated parameters  $\{\mathbf{w}_a\}_{a=1}^L$  increases while the data size  $M = \alpha N = 400$  is fixed, meaning that the problem becomes more and more underdetermined with the growth of  $L$ . Hence, Fig. 1 demonstrates that the developed approximations work irrespectively of how much the problem is underdetermined.

Fig. 2 exhibits the  $\sigma_\xi^2$ -dependence of the likelihoods and the approximation results for  $L = 8$  and  $N = 200$ . For the very weak noise case ( $\sigma_\xi^2 = 0.001$ , left), the difference between the predictive and training likelihoods is negligible and hence all four curves are not discriminable. For the moderate ( $\sigma_\xi^2 = 0.1$ , middle) and large ( $\sigma_\xi^2 = 1$ , right) noise cases, the training curve is very different from the predictive ones. The approximation curves are again consistent with the literal 10-fold one.

Fig. 3 demonstrates how the approximation accuracy changes as the system size  $N$  grows. For small sizes  $N = 50, 100$ , a discriminable difference exists between the results of the approximations and the literal 10-fold CV, as well as the difference between the results of the two approximations. This is expected, because our derivation relies on the largeness of  $N$  and  $M$ . For large systems  $N = 400, 800$ , the difference among the two approximations and the literal CV is much smaller. Considering this example in conjunction with the middle panel of Fig. 1, we can recognize that our approximate formula becomes fairly precise for  $N \geq 200$  in this parameter set.

Finally, let us consider the actual computational time to evaluate  $\{\hat{\mathbf{w}}_a\}_a$  and the approximate LOEs, and observe its system size dependence. The left panel of Fig. 4 provides the plot of the actual computational time against the system size. Here, the number of

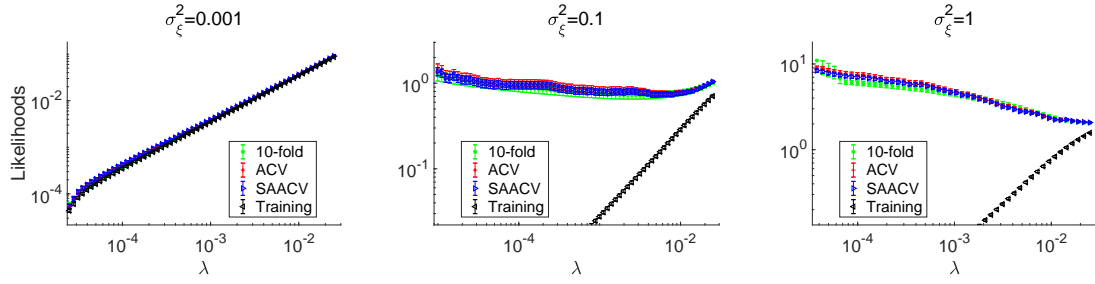


Figure 2: Log-log plots of the likelihoods against  $\lambda$  for several noise strengths. Other parameters are fixed at  $N = 200$ ,  $L = 8$ ,  $\alpha = 2$  and  $\rho_0 = 0.5$ . The approximation results are consistent with the literal 10-fold CV, irrespectively of the noise strength. The convergence threshold  $\delta$  is set to be  $\delta = 10^{-9}$  for the case  $\sigma_\xi^2 = 1$ .

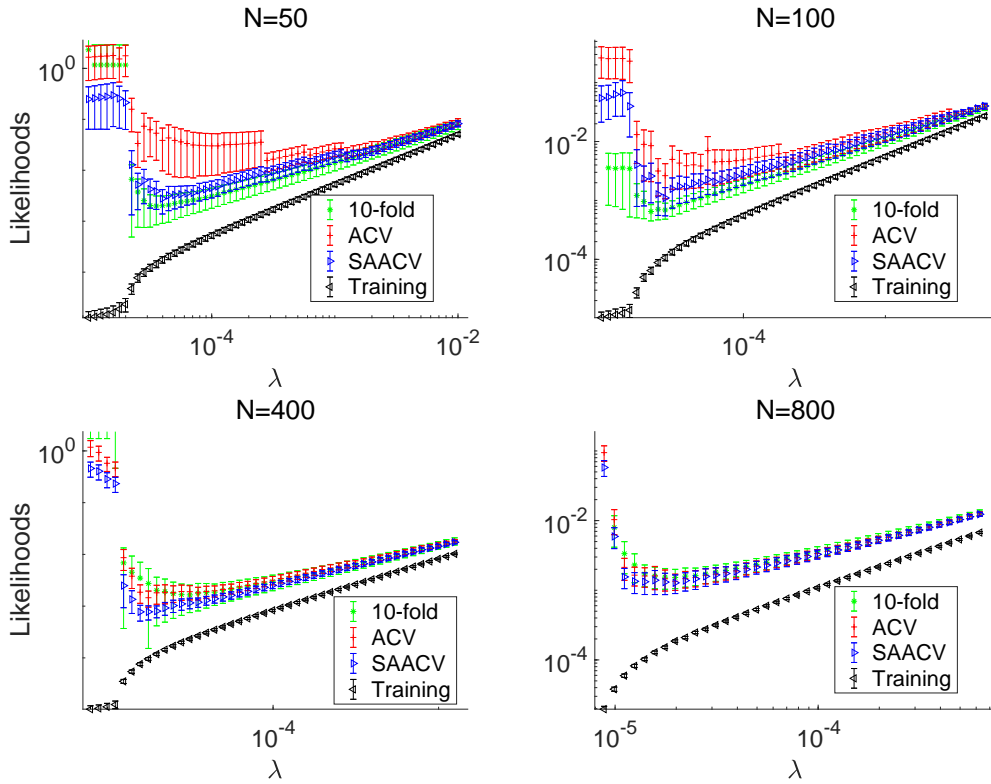


Figure 3: Log-log plots of the likelihoods against  $\lambda$  for several values of feature dimensionality  $N$ . Other parameters are fixed at  $L = 8$ ,  $\sigma_\xi^2 = 0.01$ ,  $\alpha = 2$  and  $\rho_0 = 0.5$ .

examined points of  $\lambda$  to obtain a solution path is different from size to size, and hence the plotted time is given as the whole computational time to obtain the solution path divided by the number of  $\lambda$ s points. The left panel of Fig. 4 clearly displays the advantage and

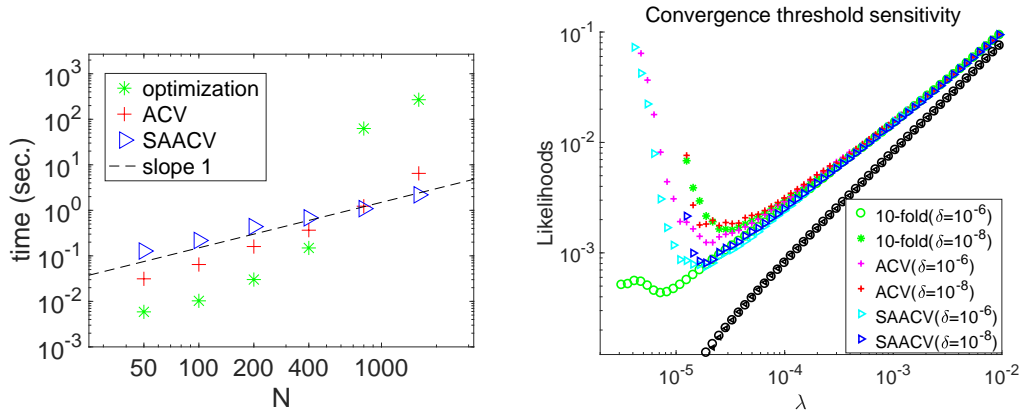


Figure 4: (Left) Actual computational time spent to find the solution of eq. (3) and that for ACV and SAACV, plotted against the feature dimensionality  $N$  in a double logarithmic scale. Note that the computational time for the  $k$ -fold CV is about  $k$  times larger than that for finding the solution of eq. (3), represented by the green asterisks. Parameters are fixed at  $L = 8$ ,  $\sigma_{\xi}^2 = 0.01$ ,  $\alpha = 2$  and  $\rho_0 = 0.5$ . (Right) The likelihoods are obtained for the two convergence thresholds  $\delta = 10^{-6}$  and  $\delta = 10^{-8}$ . Error bars are omitted for visibility. For the tighter case  $\delta = 10^{-8}$ , the minimum value of  $\lambda$  in the examined range is larger than that of the case  $\delta = 10^{-6}$ , due to computation, though the systematic difference with the results of the literal 10-fold CV is already clear. The training likelihoods of these two different  $\delta$ , represented by black circles and left-pointing triangles, are completely overlapping. The system parameters are  $N = 400$ ,  $L = 8$ ,  $\sigma_{\xi}^2 = 0.01$ ,  $\alpha = 2$  and  $\rho_0 = 0.5$ .

disadvantage of the developed approximations. For small sizes, the computational time for optimization to obtain  $\{\hat{\mathbf{w}}_a\}_a$  is shorter than the time to compute the approximate LOOE, and hence the literal CV is better. However, for larger systems, the optimization cost increases rapidly and for  $N \gtrsim 400$  the approximate CV is better. For  $N \gtrsim 800$ , the ACV cost exceeds that of SAACV. The SAACV cost behaves linearly as a function of  $N$  (see the black dashed line), and hence for larger systems of  $N \gtrsim 800$  SAACV can be a very powerful tool. As a related issue, we mention the convergence problem of the algorithm. In the right panel of Fig. 4, we compare the likelihoods at two different values of the convergence threshold  $\delta$ . An important observation is that a significant difference exists in the literal CV results while other curves do not show a strong change. This implies that our approximate formula is rather robust and can be used with a rather loose convergence threshold or conversely, we can use the systematic deviation between the literal CV and our approximations as an

indicator to verify the tightness of the convergence threshold. This is beneficial, especially when treating large models, for which the convergence check is a common annoying task.

### 3.2 On real-world dataset

Next, we test the approximate formula on a real-world dataset. As shown above, our approximations become more precise if the model dimensionality and data size are large. Hence, we chose the ISOLET dataset which is a relatively large problem among classification tasks collected in the UCI machine learning repository (Lichman, 2013). The feature dimensionality, the data size, and the class number are  $N = 617$ ,  $M = 6238$ , and  $L = 26$ , respectively. We apply a 10-fold CV and our approximations to this dataset as so far, and the result is given in Fig. 5. The results of the approximations and of the 10-fold CV demonstrate a

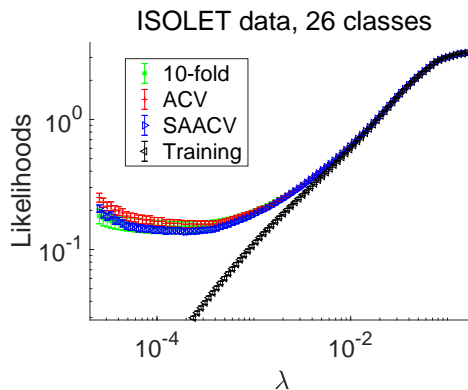


Figure 5: Approximate CV performance on the ISOLET data of  $L = 26$  classes. At the estimated minimums of the predicted likelihood, the accuracy rate for correctly classifying the test data is about 0.86 while the probability of recovering the training data is about 0.98, commonly among the literal CV and the two approximations. At the minimum value of  $\lambda$ , the leftmost point in the figure, the accuracy rates are different among the three different methods, and are 0.83, 0.78, and 0.81 for the literal CV, ACV and SAACV, respectively.

fairly good agreement, proving the actual effectiveness of the developed approximations. In an experiment, the actual computational time to obtain the result of the full simulation, of the 10-fold CV, of ACV, and of SAACV were 785, 7825, 5173, and 689 seconds, respectively. The system parameters  $\{N, M, L\}$  are rather large in this problem and thus the advantage of ACV is not large, while the efficiency of SAACV stands out in such situations.

## 4. Conclusion

In this paper, we have developed an approximate formula for the CV estimator of the predictive likelihood of the multinomial logistic regression regularized by the  $\ell_1$ -norm. We have also demonstrated their advantages and disadvantages in numerical experiments using simulated and real-world datasets. Two versions of the approximation have been defined

based on the developed formula. The first version, abbreviated as ACV, has a better performance, in terms of computational time, for middle size problems. It will eventually become worse than the literal  $k$ -fold CV with moderate  $k$ s as the problem size grows, because its computational time is scaled as a third-order polynomial of the feature dimensionality and data size,  $N$  and  $M$ , though such a tendency has not been observed in the investigated range of  $N$ . We have also defined the second version based on ACV, the computational time of which is just scaled linearly with respect to  $N$  and  $M$ . This second approximation is called SAACV, and it has been demonstrated that SAACV is slow for small size problems but has a great advantage for large size problems. Hence, we suggest leveraging the literal CV for small, ACV for middle, and SAACV for large size problems.

Our derivation is based on the perturbation that assumes that there is a small difference between the full and leave-one-out solutions. This assumption will not be satisfied for some specific cases, such as when the feature vectors are sparse. Even with this restriction, we expect the range of application of our formula is wide enough and we would like to encourage readers to leverage it in their own work.

The perturbative approach employed here is fairly general and can be applied to a wide class of generalized linear models with convex regularizations. The development of practical formulas for these cases will be of great assistance, given that we are living in the Big Data era.

## Acknowledgments

This work was supported by JSPS KAKENHI Nos. 25120013 and 17H00764.

## Appendix A. The SA approximation

Let us derive eq. (38) in the SA approximation. We work on a framework called a cavity method in statistical physics or belief propagation (BP) in computer science. We start from defining the so-called Boltzmann distribution:

$$P\left(\{\mathbf{w}_a\}_{a=1}^L \middle| D^M, \lambda\right) = \frac{1}{Z(D^M, \lambda)} e^{-\beta \mathcal{H}(\{\mathbf{w}_a\}_{a=1}^L \middle| D^M, \lambda)} = \frac{e^{-\beta \lambda \|\mathbf{w}_a\|_1}}{Z(D^M, \lambda)} \prod_{\mu=1}^M \phi^\beta(y_\mu | \{u_{\mu a}\}_a). \quad (45)$$

In the  $\beta \rightarrow \infty$  limit, this distribution converges to a point-wise measure of the solution of eq. (3) and hence, it is useful for analyzing eq. (45).

In this appendix, we introduce a new vector representation summarizing class variables:  $\mathbf{w}_i = (w_{ai})_a$ . Note that this is different from the notation used in the main body of this paper,  $\mathbf{w}_a = (w_{ai})_i$  in which the feature components are summarized.

By regarding  $\mathbf{w}_i$  as a single variable node, the BP decomposes eq. (45) into two types of messages as follows:

$$\tilde{M}_{\mu \rightarrow i}(\mathbf{w}_i) = \int \prod_{j(\neq i)} d\mathbf{w}_j \phi^\beta(\mathbf{u}_\mu) \prod_{j(\neq i)} M_{j \rightarrow \mu}(\mathbf{w}_j), \quad (46)$$

$$M_{i \rightarrow \mu}(\mathbf{w}_i) = e^{-\beta \lambda \|\mathbf{w}_i\|_1} \prod_{\nu(\neq \mu)} \tilde{M}_{\nu \rightarrow i}(\mathbf{w}_i), \quad (47)$$



where  $\mathbf{u}_\mu = (u_{\mu a})_a$ . A crucial observation to assess eqs. (46,47) is that the argument of the potential function  $\phi(\mathbf{u}_\mu)$  has a sum of an extensive number of random variables; the central limit theorem thus justifies treating it as a Gaussian variable with the appropriate mean and variance. Hence, according to eq. (46) where  $\mathbf{w}_i$  is special, we can divide the extensive sum as follows:

$$u_{\mu a} = \sum_j x_{\mu j} w_{aj} = x_{\mu i} w_{ai} + \sum_{j(\neq i)} x_{\mu j} w_{aj} \approx x_{\mu i} w_{ai} + \sum_{j(\neq i)} x_{\mu j} \langle w_{aj} \rangle^\mu + t_a, \quad (48)$$

where the second term on the right-hand side represents the mean of  $\sum_{j(\neq i)} x_{\mu j} w_{aj}$ , the symbol  $\langle \cdot \rangle^\mu$  denotes the average over the Boltzmann distribution without the  $\mu$ th potential function, and  $\mathbf{t}^\mu = (t_a^\mu)_a$  denotes the zero-mean Gaussian variables whose covariance is set to be that of  $\left( \sum_{j(\neq i)} x_{\mu j} w_{aj} \right)_a$ . This expression allows us to replace the integration  $\int \prod_{j(\neq i)} d\mathbf{w}_j$  by that over  $\mathbf{t}^\mu$  in eq. (46). This significantly simplifies the computation and yields:

$$\tilde{M}_{\mu \rightarrow i}(\mathbf{w}_i) \approx \int d\mathbf{t} e^{\beta \left( -\frac{1}{2} \mathbf{t}^\top (C_\mu^\mu)^{-1} \mathbf{t} - q_\mu(\mathbf{w}_i, \mathbf{t}) \right)} \equiv \int d\mathbf{t} e^{\beta f^\mu(\mathbf{w}_i, \mathbf{t})} \quad (49)$$

where  $q_\mu(\mathbf{w}_i, \mathbf{t}) = -\ln \phi(\mathbf{u}_\mu)$  and  $C_\mu^\mu$  is the rescaled covariance of  $\sum_{j(\neq i)} x_{\mu j} w_{aj}$  defined as

$$\begin{aligned} \chi_{(ai)(bj)}^\mu &\equiv \beta \left( \langle w_{ai} w_{bj} \rangle^\mu - \langle w_{ai} \rangle^\mu \langle w_{bj} \rangle^\mu \right), \\ (C_\mu^\mu)_{ab} &\equiv \sum_{i,j} x_{\mu i} x_{\mu j} \chi_{(ai)(bj)}^\mu. \end{aligned} \quad (50)$$

In the second equation we added the contribution from  $i$  for simplicity. It does not affect the following result because the  $i$ th term contribution is small enough. Let us focus on the limit  $\beta \rightarrow \infty$ . This limit allows us to use the saddle-point method with respect to  $\mathbf{t}^\mu$ . The associated saddle-point equation is:

$$\hat{\mathbf{t}}^\mu = -C_\mu^\mu \mathbf{b}^\mu(\mathbf{w}_i, \hat{\mathbf{t}}^\mu), \quad (51)$$

where  $\mathbf{b}^\mu$  is the gradient of  $q_\mu$  with respect to  $\mathbf{u}_\mu$  defined at eq. (12). Now, let us expand the exponent  $f^\mu(\mathbf{w}_i, \mathbf{t})$  in eq. (49) with respect to the dynamical variables  $\mathbf{w}_i$  up to the second order. Putting  $z_a = \sum_i x_{\mu i} w_{ai}$ , we can define the derivatives as:

$$\frac{\partial \hat{\mathbf{t}}^\mu}{\partial z_a} = -(I_L + C_\mu^\mu F^\mu)^{-1} C_\mu^\mu F_{*a}^\mu, \quad (52)$$

$$\frac{\partial f^\mu(\mathbf{w}_i, \hat{\mathbf{t}}^\mu)}{\partial z_a} = -b_a^\mu(\mathbf{w}_i, \hat{\mathbf{t}}^\mu), \quad (53)$$

$$\frac{\partial^2 f^\mu(\mathbf{w}_i, \hat{\mathbf{t}}^\mu)}{\partial z_a \partial z_b} = -F_{ab}^\mu - \left( \frac{\partial \hat{\mathbf{t}}^\mu}{\partial z_a} \right)^\top F_{*b}^\mu = - \left( \left( I_L + F^\mu C_\mu^\mu \right)^{-1} F^\mu \right)_{ab}. \quad (54)$$

Hence,

$$\tilde{M}_{\mu \rightarrow i}(\mathbf{w}_i) \propto e^{\beta \left( \mathbf{h}_i^\mu \mathbf{w}_i - \frac{1}{2} \mathbf{w}_i^\top \Gamma_i^\mu \mathbf{w}_i \right)} \quad (55)$$

where

$$\begin{aligned} h_i^\mu &= -x_{\mu i} \mathbf{b}^\mu, \\ \Gamma_i^\mu &= x_{\mu i}^2 (I_L + F^\mu C_\mu^\backslash\mu)^{-1} F^\mu. \end{aligned} \quad (56)$$

Note that this second order expansion is justified in the limit  $\beta \rightarrow \infty$ .

Collecting all the messages except for  $\mu$ , we can construct the LOO marginal distribution of  $\mathbf{w}_i$  as:

$$P^{\backslash\mu}(\mathbf{w}_i) \propto e^{-\beta\lambda\|\mathbf{w}_i\|_1} \prod_{\nu(\neq\mu)} \tilde{M}_{\nu\rightarrow i}(\mathbf{w}_i) \propto e^{\beta((\sum_{\nu(\neq\mu)} \mathbf{h}_i^\nu)\mathbf{w}_i - \frac{1}{2}\mathbf{w}_i^\top (\sum_{\nu(\neq\mu)} \Gamma_i^\nu)\mathbf{w}_i - \lambda\|\mathbf{w}_i\|_1)}. \quad (57)$$

Now, we can close the equation for the rescaled variance  $(\chi_i^{\backslash\mu})_{ab} \equiv \chi_{(ai),(bi)}^{\backslash\mu}$ , because we can compute the variance of  $\mathbf{w}_i$  from eq. (57). By considering the scaling, we can recognize that the variances vanish in the speed of  $O(\beta^{-2})$  if one of the two components or both are inactive. The active-active components of the variance are scaled by  $O(\beta^{-1})$  and remain in the rescaled variance. Focusing on the limit  $\beta \rightarrow \infty$ , we thus obtain:

$$(\chi_i^{\backslash\mu})_{\hat{A}_i \hat{A}_i} = \left( \left( \sum_{\nu(\neq\mu)} \Gamma_i^\nu \right)_{\hat{A}_i \hat{A}_i} \right)^{-1} \approx \left( \left( \sum_{\nu} \Gamma_i^\nu \right)_{\hat{A}_i \hat{A}_i} \right)^{-1}. \quad (58)$$

At the last step, the  $\mu$ th term is added since its contribution is expected to be small enough in the summation. This manifests that the  $\mu$ -dependence of  $\chi^{\backslash\mu}$  can be neglected and we rewrite it as  $\chi^{\backslash\mu} = \chi$  hereafter. By considering the meaning of the Hessian, it is easy to understand that  $G^{\backslash\mu}$  is identified with  $(\sum_{\nu(\neq\mu)} \Gamma_i^\nu)$ . This yields eq. (37).

By assuming the vanishing correlation between  $\mathbf{w}_i$  and  $\mathbf{w}_j$  for  $i \neq j$ , we can write

$$\chi_{(ai)(bj)} \approx \delta_{ij} \begin{cases} (\chi_i)_{ab} & (a, b \in \hat{A}_i) \\ 0 & (\text{otherwise}) \end{cases}. \quad (59)$$

These leads to:

$$(C_\mu^{\backslash\mu})_{ab} = \sum_{ij} x_{\mu i} x_{\mu j} \chi_{(ai)(bj)}^{\backslash\mu} \approx \sum_i x_{\mu i}^2 (\chi_i)_{ab} \approx \sigma_x^2 \sum_i (\chi_i)_{ab} \equiv (C_{\text{SA}})_{ab} \quad (60)$$

The  $\mu$ -dependence through  $x_{\mu i}^2$  is neglected at the last step, because the sum  $\sum_i$  would mask such a weak  $\mu$ -dependence. Similarly, we may write the sum inside the parentheses of the righthand side of eq. (58) as:

$$\sum_{\nu} \Gamma_i^\nu \approx \sigma_x^2 \sum_{\nu} (I_L + F^\nu C_{\text{SA}})^{-1} F^\nu. \quad (61)$$

Inserting eqs. (59-61) into eq. (58), we obtain eq. (38).

Careful readers may be concerned about the neglected  $\mu$ -dependence of  $\chi^{\backslash\mu}$ , as well as that of  $G^{\backslash\mu}$ . If this can be neglected, may we replace  $G^{\backslash\mu}$  with  $G$  from the beginning at eq. (19)? The answer is of course no. The reason is that the difference between  $G^{\backslash\mu}$  and  $G$

is not negligible if they are “projected” onto  $X^\mu$  as in eq. (19). If they are projected onto other directions perpendicular to  $X^\mu$ , the difference is actually tiny and can be neglected, but for computing the factor  $C_\mu^{\setminus\mu}$  we need to take into account this difference appropriately. This results in the additional factor  $(I - F_\mu C_\mu)^{-1}$  in eq. (21). In the SA approximation, the factor  $C$  is computed based on neglecting the difference between  $G$  and  $G^{\setminus\mu}$ . As a result we cannot discriminate the two factors  $C_\mu$  and  $C_\mu^{\setminus\mu}$ . This consideration implies that our SA estimation of  $C$ ,  $C_{SA}$ , should be applied to  $C_\mu^{\setminus\mu}$  in eq. (19) and should NOT be applied to  $C_\mu$  in eq. (21), because the latter formula formally takes into account the difference in advance.

## References

- Tomohiro Ando and Ruey Tsay. Predictive likelihood for bayesian model selection and averaging. *International Journal of Forecasting*, 26(4):744–763, 2010.
- Jan F Bjornstad. Predictive likelihood: a review. *Statistical Science*, pages 242–254, 1990.
- Jerome Friedman, Trevor Hastie, and Rob Tibshirani. Regularization paths for generalized linear models via coordinate descent. *Journal of statistical software*, 33(1):1, 2010.
- Balaji Krishnapuram, Lawrence Carin, Mario AT Figueiredo, and Alexander J Hartemink. Sparse multinomial logistic regression: Fast algorithms and generalization bounds. *IEEE transactions on pattern analysis and machine intelligence*, 27(6):957–968, 2005.
- M. Lichman. UCI machine learning repository, 2013. URL <http://archive.ics.uci.edu/ml>.
- Tomoyuki Obuchi and Yoshiyuki Kabashima. Cross validation in lasso and its acceleration. *Journal of Statistical Mechanics: Theory and Experiment*, 2016(5):53304–53339, 2016.
- Tomoyuki Obuchi, Shiro Ikeda, Kazunori Akiyama, and Yoshiyuki Kabashima. Accelerating cross-validation with total variation and its application to super-resolution imaging. *arXiv preprint arXiv:1611.07197*, 2016.
- Manfred Opper and Ole Winther. A mean field algorithm for bayes learning in large feed-forward neural networks. In *Advances in Neural Information Processing Systems*, pages 225–231, 1997.
- Mark Schmidt. Graphical model structure learning with l1-regularization. *University of British Columbia*, 2010.
- Hastie Trevor, Tibshirani Robert, and Friedman Jerome. *The Elements of Statistical Learning; Data Mining, Inference, and Prediction*. Springer-Verlag New York, 2009. doi: 10.1007/978-0-387-84858-7.